Article

Development of Epigallocatechin and Ascorbic Acid Dual Delivery Transferosomes for Managing Alzheimer's Disease: In Vitro and in Vivo Studies

Gaurav Mishra, Rajendra Awasthi, Sunil Kumar Mishra, Anurag Kumar Singh, Anurag Kumar Tiwari, Santosh Kumar Singh, and Manmath K. Nandi*

Read Online

ACCESS | Metrics & More | Article Recommendations

ABSTRACT: Epigallocatechin-3-gallate (EGCG) and ascorbic acid (AA)-loaded transferosomes (TRANS) were developed for brain delivery. The investigation covered EGCG-TRANS, AA-TRANS, and EGCG-AA-TRANS formulations using the film hydration technique. We analyzed the formed transferosomes to confirm the presence of vesicles loaded with the respective drugs and their performance within a living organism. The sizes of the particles for EGCG-TRANS, AA-TRANS, and EGCG-AA-TRANS were measured correspondingly at 174.2 ± 1.80, 132.7 ± 12.22, and 184.31 ± 9.5 nm. The appearance of diffused rings in the scanning electron microscopic image suggests that the payload has a crystalline structure. The atomic force microscope image displayed minimal surface irregularities, potentially indicating the presence of a lipid layer on the surface. Hemolysis results indicated the safety of the vesicles. The results showed 10.23, 7.21, and 8.20% of hemolysis for EGCG-TRANS, AA-TRANS, and EGCG-AA-TRANS, respectively. In the case of EGCG-AA-TRANS, the release of EGCG was determined to be $61.65\% \pm 4.61$ after 72 h when exposed to phosphate buffer saline (pH 7.4). In vivo studies show a good response against Alzheimer's disease (AD). EGCG-AA-TRANS (82.166%) exhibited a higher percentage of AChE inhibition in comparison to EGCG-TRANS (66.550%) and AA-TRANS (53.466%). Intranasal delivery of EGCG-AA-TRANS resulted in approximately a 5-fold enhancement in memory. Formulation allowed EGCG and AA to accumulate in various organs, including the brain. The results suggest that EGCG-AA-TRANS could be safe and effective for treating AD.
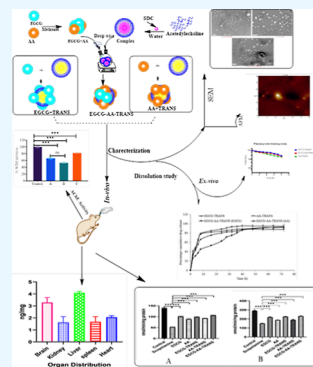
1. INTRODUCTION

Alzheimer's disease (AD) accounts for 60−80% of reported dementia cases globally. It manifests as dementia and, eventually, the impairment of normal activities like swallowing or regular working, which ultimately trend toward fatality.[1,2] AD is the seventh leading cause of death worldwide, resulting in the mortality of about 55.2 million individuals worldwide. It is assumed that by 2050, approximately 139 million people will be affected by dementia. Approximately 65% of dementia-related fatalities occur in women. In 2016, the estimated per patient cost of formal care was USD 28,078, and the value of informal care in terms of replacement cost and forgone wages was USD 36,667 and USD 15,792, respectively. Aggregate formal care costs and formal plus informal care costs using replacement cost and forgone wage methods were USD 196 billion, USD 450 billion, and USD 305 billion, respectively, in 2020. Projections for 2060 predict increases of USD 1.4 trillion, USD 3.3 trillion, and USD 2.2 trillion, respectively.[3] Although the frequency of AD increases with age, the exact causes remain unknown. The primary scientific explanation focuses on alterations in the process of amyloid formation and the hyperphosphorylation of specific brain proteins (Tau). This theory is based on the increased aggregation of Aβ plaques and the beginning of neurofibrillary tangle production in the brain. Both processes can result in the death of neuronal tissue, followed by the development of dementia.[4] Recent investigations have documented that disruptions in these pathways are associated with the initiation of the disease. In addition, other physiological changes, including disruptions in cholesterol homeostasis, insulin signaling, neuroinflammation, mitochondrial function, and oxidative stress, have been identified as factors contributing to the complex development of AD.[5]

Due to the unknown causes of AD and the delayed onset of initial symptoms, early diagnosis and identification of effective therapies are challenging.[6,7] Donepezil, rivastigmine, and galantamine are the only approved cholinesterase inhibitors for AD management. Memantine is the first approved *N*-
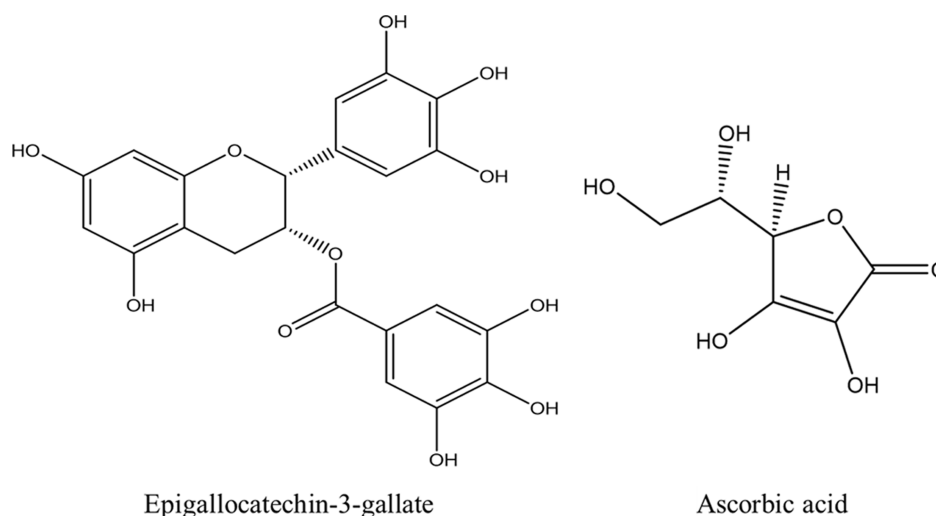
Figure 1. Chemical structure of epigallocatechin-3-gallate and AA.

methyl-D-aspartic acid receptor antagonist used in the treatment of AD. These treatments are efficacious for patients in the mild-to-moderate and moderate-to-severe phases of the condition, respectively.[8] However, as these approved drugs do not halt disease progression, there is an urgent need for innovative therapeutic strategies to address this issue. Green tea stands out as a globally favored beverage, renowned for its potential to bolster well-being.[9] The well-known anti-inflammatory and antioxidant properties of the drink contribute to its image as a health-enhancing option. It has a beneficial effect on a variety of human illnesses, including metabolic syndrome, obesity, inflammatory diseases, and neurological disorders. These health benefits are derived from a class of polyphenolic compounds called catechins present in green tea.

Epigallocatechin-3-gallate (EGCG) is the most popular owing to its abundant presence and highly potent effects. However, a significant obstacle to the utilization of EGCG for human health is its poor absorption and bioavailability.[6−10] Methylation, sulfation, and glucuronidation are the main processes involved in the metabolism of green tea catechins in the intestine and liver. A substantial portion of catechins is degraded by colonic microflora, reabsorbed into the blood-stream, and excreted through urine. Ascorbic acid (AA) has demonstrated the potential to promote cellular growth while mitigating oxidative stress. The chemical structures of EGCG and AA are illustrated in Figure 1. Recent studies have shown promising outcomes by administering EGCG and AA, leading to enhanced therapeutic advantages in treating AD.[11,12]

Single-molecule-targeting approaches could lead to unin-tended effects on nontargeted sites. This could restrict the application of single-molecule targeting, especially in complex clinical conditions. Due to the presence of the blood–brain barrier (BBB), successful penetration and sustained presence of nanocarriers within diseased brain tissues might not be ensured solely through a single-molecule-targeting approach. Combining EGCG and AA for treating AD may present a promising approach due to their complementary mechanisms of action and synergistic effects on brain health, such as antioxidant properties, neuroprotective effects, and anti-inflammatory activity. EGCG has been shown to inhibit the aggregation of beta-amyloid proteins, which form plaques in the brains of Alzheimer's patients.[13] AA, on the other hand,

can enhance the clearance of beta-amyloid from the brain and increase the bioavailability of EGCG by stabilizing its molecular structure.[14]

Nanomedicines have great potential as topical drug delivery carriers. Transferosomes, a unique type of vesicle, consist of concentric layers of phosphatidylcholine, cholesterol, and an edge activator with an aqueous or ethanolic core. Phosphati-dylcholine is the primary phospholipid present in eukaryotic cell membranes. As a result, it reduces the likelihood of adverse consequences and makes it acceptable for drug delivery to sensitive areas. Edge activators have remarkable deformability and flexibility, allowing them to easily pass through the biological membranes.[15] In a recent study, Mirza et al. reported improved brain targeting efficiency of cefepime-loaded trans-ferosomes via the intranasal route.[16] Salem et al. developed donepezil hydrochloride-loaded nanotransferosomes for the treatment of AD. These nanotransferosomes were nontoxic, tolerable, and had a high nose-to-brain transport percentage (80.32%).[17] Gupta et al. reported naringin-loaded trans-niosomes for the treatment of epilepsy. The developed transniosomes had permeation across the nasal mucosa, and intranasally administered transniosomes had a greater C_{max} and $AUC_{0−24}$ h than orally administered transniosomes.[18]

2. MATERIAL AND METHODS

2.1. Materials. EGCG was procured from Sigma-Aldrich, Mumbai, India. Span 60 was purchased from Sigma-Aldrich (Mumbai, India). AA was procured from SD Fine Chem., Mumbai, India. Sigma-Aldrich Chemie GmbH (Munich, Germany) provided dialysis cellulose membrane (molecular weight cut off 12,000 g/mol). The EMD Millipore Company (Cork, Ireland) supplied membrane filters. SISCO Research Laboratories (Mumbai, India) provided potassium dihydrogen phosphate and disodium hydrogen phosphate. Xylene was obtained from El-Nasr Pharmaceutical Co. (Cairo, Egypt). Carbon-coated TEM grids (CF300-Cu) were obtained from EMS (Hatfield, PA). Sigma-Aldrich (St. Louis, MO) supplied the acetylcholinesterase activity assay kit (Cat. no. MAK119). Sodium deoxycholate (SDC) was supplied by SD Fine Chemicals (Mumbai, India). Merck (Darmstadt, Germany) supplied potassium dichromate and hydrogen peroxide (protein estimation kit, Bradford GeNei). Sisco Laboratory Limited (Mumbai, India) provided ammonium chloride, acetic
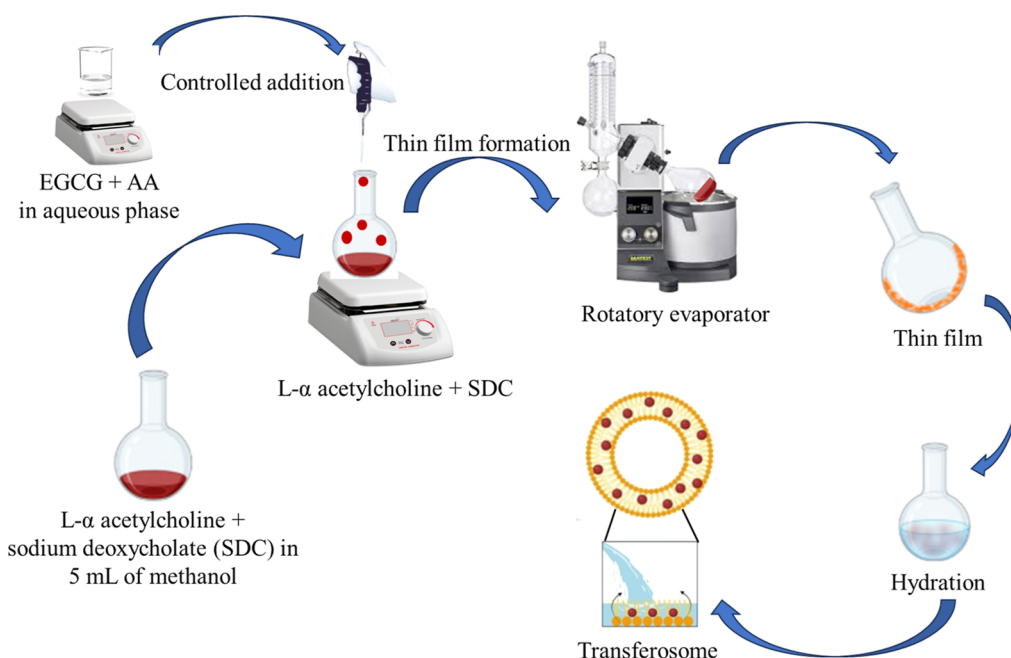
Figure 2. Schematic presentation of epigallocatechin and/or AA-loaded dual delivery transferosome preparation by the thin-film hydration technique. Created with BioRender.com.

acid, sodium dihydrogen phosphate, disodium hydrogen phosphate, and potassium chloride.

2.2. Methods. *2.2.1. Preparation of EGCG/AA-Loaded Transferosomes.* Thin film hydration was used to prepare EGCG and/or AA-loaded transferosomes. SDC (1 mg) and L-α phosphatidylcholine (100 mg) were taken in the RBF (round-bottom flask). 5 mL of CH_3OH (methanol) was poured into the flask containing SDC and L-α phosphatidylcholine and stirred at 100 rpm using a magnetic stirrer at 37 $\pm$ 1 °C. Powdered samples of EGCG/AA (5 mg each) were dissolved in 2 mL of an aqueous phase. The EGCG/AA mixture was added dropwise (1 mg per minute) to the RBF containing SDC and L-α phosphatidylcholine. The solution was stirred for 10 min and subjected to sonication for 5 min (20 s on and 20 s off) using a probe sonicator (Hielscher UP400ST Ultrasonic Processor). The solution was placed under reduced pressure at a temperature of 60 °C using a rotary film evaporator until a dry film was obtained. For the hydration of dry film, 10 mL of Milli-Q water was added. The obtained transferosomal suspension was stored in an airtight glass storage bottle after completing film hydration in a rotary evaporator under reduced pressure.[19] Figure 2 illustrates the schematic presentation of EGCG and/or AA-loaded transferosomes dual delivery transferosomes prepared by the thin-film hydration technique.

2.2.2. In Vitro Characterization of Prepared Transferosomes. 2.2.2.1. Determination of Size, Polydispersity Index, Zeta Potential, Drug Loading, and Entrapment Efficiency. DLS measurements were done using a Nano ZS zeta sizer (Malvern Instruments, Malvern, U.K.) to determine the hydrodynamic diameter, zeta potential (ζ), and polydispersity index (PDI) of EGCG-AA-TRANS. To prevent contamination, water free from microbes was used as the dispersion medium to prepare the samples. The DLS analysis was performed within a scattering angle range of 40 to 150°, with a 6° interval, using a refractive index of 1.10. A probe sonicator (Hielscher UP400ST Ultrasonic Processor) was used

to sonicate the sample. The distribution intensity of the scattered light was measured to calculate the hydrodynamic diameter of the particles. Laser Doppler velocimetry was used to estimate ζ values. For each sample, an average measurement of twice was recorded to determine the ζ. The instrument was set with a diode laser to analyze size distribution.[20]

Encapsulation efficiency (% EE) and drug loading (% DL) of EGCG-TRANS, AA-TRANS, and EGCG-AA-TRANS were estimated by the passive method. 5 milligram sample was dispersed in Milli-Q water (5 mL), followed by centrifugation (C-24BL, REMI, Maharashtra, India) at 10,000 rpm for 30 min. The supernatant was examined at 496 and 520 nm for EGCG and AA, respectively, using a UV spectrophotometer (LT-2800, Labtronics, India). The percentages of encapsulation efficiency (% EE) and drug loading (% DL) were computed using the following equations[21,22]

$$DL\ (\%) = \frac{\text{amount of drug taken} - \text{unentraped drug}}{\text{ammount of loaded drug}} \times 100$$

$$EE\ (\%) = \frac{\text{amount of drug taken} - \text{unentraped drug}}{\text{ammount of drug taken}} \times 100$$

2.2.2.2. Morphological Characterization. High-resolution scanning electron microscopy (SEM) (Nova Nano SEM 450 (FEI) instrument, Singapore) was used to examine the shapes of EGCG-TRANS, AA-TRANS, and EGCG-AA-TRANS. Atomic force microscopy (AFM) was conducted using an NTEGRA Prima system (NT-MDT Service & Logistics Ltd., Ireland) for 2D and 3D surface analysis of the transferosomes. The scanning electron microscope (Nova Nano SEM 450) was equipped with a Team Pegasus integrated energy-dispersive spectrometer featuring Octane Plus and Hikari Pro detectors from Tokyo, Japan. SEM enabled both morphological and dimensional characterization of the drug-loaded transferosomes. Prior to imaging, the samples were dried in a

microprocessed oven at 45 °C for 30 min. To enhance imaging quality, a gold coating was applied to the samples using a 7620 EMS SEM sputter coater. Images were captured at an acceleration voltage of 200 kV using an extra-large-view III CCD camera.[23]

2.2.2.3. In Vitro Release Study for Drug Release. The investigation of in vitro release patterns of EGCG and AA from EGCG-TRANS, AA-TRANS, and EGCG-AA-TRANS was done by the dialysis bag technique (with a molecular weight cutoff of 5000 Da, an average flatness of −50, a diameter of 14.3 mm, a width of 22.56 mm, and a capacity of 1.6 mL/cm, procured from HiMedia, India). A methanolic solution of EGCG (1000 μg) and AA (1000 μg) was placed into separate dialysis bags. Similarly, separate dialysis bags were filled with EGCG-TRANS particles (≈1 mg of EGCG), AA-TRANS particles (≈1 mg of AA), and EGCG-AA-TRANS particles (≈1 mg of EGCG and 1 mg of AA). The temperature of the release media (100 mL of phosphate buffer saline, PBS—pH 7.4) was maintained at 37 ± 0.5 °C. At predetermined intervals, 2 mL aliquots were withdrawn, and an equivalent volume of fresh medium at the same temperature was replenished to maintain the sink condition. The quantification of EGCG and AA release was done at 496 and 520 nm, respectively, using a UV–vis spectrophotometer (Nanodrop ND1000, Thermo Scientific, Wilmington).[24]

2.2.3. Ex Vivo Analysis. 2.2.3.1. Acetylcholinesterase Inhibitory Activity. Acetylcholinesterase (AChE) activity assay was conducted in an in vitro setting using sodium phosphate assay buffer (pH 7.5). The experiment was carried out using a microplate reader (BMG Labtech, Ortenberg, Germany). The protocol outlined in the AChE test kit was followed to prepare AChE solution (Sigma-Aldrich Co., MO, Cat. no. MAK119). For the inhibitory test, 10 mL each of EGCG-TRANS, AA-TRANS, and EGCG-AA-TRANS were used, along with 190 μL of kit reagent. The inhibitor solution was prepared as a stock solution with 20 μM sodium phosphate assay buffer (pH of 7.5). AChE activity was measured using a 1 M solution of the inhibitor. For each reaction, 200 μL of sodium phosphate assay buffer containing 2 mg of kit reagent was employed. The samples were subjected to an incubation period of 1 h at 25 °C. The absorbance of samples was recorded at 412 nm.[25]

2.2.3.2. Determination of Hemolytic Toxicity. Hemolytic toxicity studies of pure EGCG and AA, EGCG-TRANS, AA-TRANS, and EGCG-AA-TRANS were done with slight modifications from the reported protocol.[17] From a healthy subject, 8 mL of whole blood was collected and stored in an EDTA-coated vial. The blood samples were suspended in a normal saline solution (0.9% w/v). The suspension was subjected to centrifugation at 2200 rpm and 25 ± 2 °C using a cooling centrifuge (R-4C DX, REMI, Maharashtra, India). A sample (20 ppm) was prepared by diluting it in saline. 4 mL of each prepared sample were added to red blood cells (RBCs) and set aside for a period of time to allow for interaction and potential RBC rupture. After 1 h incubation, samples were centrifuged. The supernatant was analyzed using a UV–visible spectrophotometer at 540 nm.[26] As a control, RBCs suspended in distilled water were used. This control sample established a baseline for comparison with the experimental samples. The percentage of hemolysis (rupture of RBCs) was calculated using the below formula

$$\text{hemolysis (\%)} = \frac{\text{absorbance of sample}}{\text{absorbance of the formulation} - \text{free control}} \times 100$$

2.2.4. In Vivo Analysis. 2.2.4.1. Experimental Animals. Swiss albino mice (30 ± 5 g) were used for the biological evaluation. Animal experimentation was done as per the guidelines provided by the Committee for Control and Supervision of Experiments on Animals (CCSEA), India. The experimental protocol was approved by the Central Institutional Animal Ethics Committee of Banaras Hindu University, Varanasi, India (Dean/2021/CEC/3051). The animals were housed in clean polypropylene cages with regular 12 h light/dark cycles. The mice had free access to a standard mouse pellet diet and water. Before the trial began, the animals (four mice per cage) were habituated to the laboratory environment.

2.2.4.2. Protocol. Animals were divided into seven groups ($n = 5$). The control group had only water and a standard diet. Scopolamine (0.5 mg/kg bw) was intranasally administered to the second group. The third group of animals received EGCG (0.5 mg/kg bw). The fourth group of animals received AA (0.5 mg/kg bw). Group five animals received EGCG-TRANS (equivalent to 0.5 mg/kg bw EGCG). Animals of group six received AA-TRANS (equivalent to 0.5 mg/kg bw AA), and the animals of the seventh group received EGCG-AA-TRANS (equivalent to 0.25 mg/kg bw of each EGCG and AA) intranasally. Treatment was given for a period of 6 days. On day seven, the treated animals received scopolamine dosing 30 min before starting trials.

2.2.4.3. Behavioral Studies. The locomotor study used Morris water-maze and Y-maze tests: Morris Water−Maze test: Over the course of 5 days, learning and memory were evaluated using the Morris water-maze test. A circular white metal pool (50 cm high, 160 cm wide) with a maintained water level of 26 cm and a temperature of 22 ± 1 °C was used for this study. Water maze software divided the water pool into four equal quadrants. The middle of the northwest quadrant (below 1.5 cm of the water surface) had a searching point that is a translucent acrylic platform (24 cm in height and 12 cm in diameter). 30 minutes before starting the trial, the animals received scopolamine. Time spent in quadrants and entries in arms were recorded in experimental mice.[27]

Y-Maze test: The Y-maze assesses working memory performance by observing spontaneous alternation. The Y-maze consists of three arms arranged horizontally in a labyrinth shape, measuring $40 \times 4.5 \times 12$ cm^3 with a 120° angle. The walls and floors in the dark environment are constructed from opaque polyethylene plastic. Mice were initially placed in one arm, followed by another in a pattern like 123,213, and so on. The manual recording of the animals' movement into different arms within the initial 5 min period was conducted. Successful alternations were defined as sequential entries into a fresh arm before revisiting the two arms already explored. Prior to every trial, a thorough cleaning of the labyrinth was done to eliminate any stains or odors. The scopolamine was given to the animals 30 min prior to the start of the experiment. The calculation of the alternation percentage was done using the below equation[28]

$$\text{alteration (\%)} = \left(\frac{\text{number of alteration}}{\text{total number of arm entries}} - 2 \right) \times 100$$

Table 1. Results Shown for PDI, ζ Potential, Particle Size Analysis, Drug Loading, and Entrapment Efficiency of EGCG-TRANS, AA-TRANS, and EGCG-AA-TRANS (Mean $\pm$ SD, n = 3)[a]

formulation code	PDI	zeta potential	particle size (nm)	entrapment efficiency (%)	drug loading (%)
EGCG-TRANS	0.064	−19.13 ± 0.41	174.2 ± 1.80	76.11 ± 3.3	14.01 ± 0.5
AA-TRANS	0.070	−22.14 ± 0.98	132.7 ± 12.22	80.13 ± 3.9	16.34 ± 2.8
EGCG-AA-TRANS	0.181	−14.21 ± 0.01	184.31 ± 9.5	82.27 ± 4.8*	15.08 ± 1.5*
				74.81 ± 4.1**	12.51 ± 1.7**

[a]*AA and **EGCG.

2.2.4.4. Biochemical Parameters. Following a painless decapitation, the animals underwent cervical dislocation. Subsequently, animal brains were dissected under cold conditions for biochemical analysis. The hippocampus was separated and preserved at −20 °C. Tissue homogenization was done with KCl buffer of pH 8.0 (140 mM NaCl, 10 mM Tris HCl, 0.5% Triton-X 100, 300 mM KCl, and 1 mM ethylenediaminetetraacetic acid) and protease and phosphatase inhibitors. The homogenates were centrifuged at 10,000 g for 25 min at 4 °C to collect the supernatant. This supernatant was then analyzed for nitrite and lipid peroxidation levels and antioxidant enzyme activities such as catalase and SOD (superoxide dismutase).[29,30]

Lipid peroxidation: The lipid peroxidation value was ascertained by the method reported by Ohkawa and co-workers, with a slight modification. The process involved combining a 10% homogenate with 10% SDS, followed by the addition of 20% acetic acid. Further, 0.8% TBA was introduced to the mixture and heated at 100 °C for 60 min using a water bath. After cooling, the assay mixture was centrifuged to collect the supernatant. The absorbance was recorded at 532 nm in relation to the control group. The extent of lipid peroxidation was quantified using malondialdehyde (MDA) micromoles per milligram of protein.[31]

NO test: Ammonium chloride and Griess reagent were combined with a 10% hippocampus homogenate. The mixture was kept at 37 °C for 90 min. The absorbance was measured at 540 nm. To establish a standard reference, a plot was created using sodium nitrite concentrations ranging from 10 to 100 mM. The nitrite content was quantified in μM/mL.[32]

2.2.4.5. SOD and Catalase Estimation. Estimation of the antioxidant enzyme activity: A UV−visible spectrophotometer was used to measure the catalase activity (n mol/min/mg protein) at 570 nm by estimating the rate of hydrogen peroxide degradation in the substrate. The hippocampal homogenate was combined with potassium dichromate and acetic acid (1:3). It was kept on a boiling water bath for 10 min. The optical density (OD) was recorded at 570 nm. For evaluating SOD activity, reduced nicotinamide adenine dinucleotide was employed as the substrate. Absorbance at 560 nm was recorded for both test and control tubes relative to a blank. The enzyme's ability to hinder nitro blue tetrazolium chloride (NBT) reduction was exhibited by calculating the OD difference between experimental and control samples. Protein quantification was performed on the enzyme source. The SOD enzyme's activity unit was defined as the amount of enzyme/mg of protein required to inhibit 50% of NBT OD within 1 min at 560 nm.[33]

2.2.4.6. Organ Distribution Study. The animals were euthanized with proper precautions by the cervical dislocation method. The brain was cleaned with normal saline and subjected to crushing and vortexing to ensure thorough homogenization. Quantification of the drugs was done using a reverse-phase high-performance liquid chromatography (HPLC) method.[34] To extract the drug content from the crushed brain, a cold centrifugation process was employed at 4 °C using a REMI C-24BL centrifuge. After centrifugation, the supernatant was separated from the brain tissue. The brain was weighed, and a portion of it was mixed with ice-cold saline solution at a specific ratio (1:10). The resulting mixture was homogenized while being maintained at a low temperature. The subsequent extraction of the brain aliquot was done using acetonitrile through a liquid−liquid extraction process, followed by vortexing for 1 min. The samples were centrifuged for 20 min using a REMI C-24BL centrifuge at 4000 rpm and 4 °C and analyzed by HPLC.[35]

2.2.4.7. Hematological Study. Animals received a consistent diet. Group I mice (control) received a regular diet. Group II mice received EGCG-TRANS (IV 0.5 mg/kg/day bw). Group III mice were treated with AA-TRANS (IV 0.5 mg/kg/day bw). Group IV mice were treated with EGCG-AA-TRANS (≈0.25 mg/kg/day bw EGCG and AA). Dosing was done for 7 days. Blood samples collected after 7 days by cardiac puncture were analyzed for a complete blood count.[36,37]

2.2.4.8. Statistical Analysis. A one-way ANOVA was executed using GraphPad Prism software (version 5.00, GraphPad Software Inc., San Diego, CA) by employing the Newman−Keuls multiple comparison test. A P value of <0.001 was considered statistically significant.

3. RESULTS AND DISCUSSION

3.1. Characterization of EGCG-TRANS, AA-TRANS, and EGCG-AA-TRANS. The polydispersity index (PDI) is used to assess the width of the size distribution in a dispersed system. An acceptable PDI value for a well-dispersed system is typically less than 0.7. A PDI value greater than 0.1 suggests a polydisperse system, while a PDI value less than 0.1 indicates a monodisperse system.[38] EGCG-AA-TRANS had a low PDI value (0.181), which suggests that the formulation has evenly distributed particles (polydisperse). The PDI value of EGCG-TRANS (0.064) was found to be lower than that of AA-TRAN (0.070), which means that EGCG-TRANS particles are more uniform in size. Both AA-TRAN and EGCG-TRANS particles formed a monodisperse system. There was the intercalation of hydrophilic and lipophilic drugs in these vesicles' aqueous compartment and lipid bilayer, respectively.[39] The entrapment efficiency of a drug in liposomal vesicles depends on its solubility characteristics. Lipophilic drugs tend to be easier to trap in the lipid bilayers of the vesicles, while hydrophilic drugs may need extra steps or changes to improve their encapsulation, depending on the surface area of the vesicles, the method of preparation, and the polymer used.[39,40] Excessive levels of surfactant (specifically SDC, which is a hydrophilic surfactant) may form porous vesicles. This phenomenon caused a reduction in the entrapment efficiency

of the vesicles, attributed to the undesired outcome of the loaded drug being released from the vesicles. Therefore, the suggested amount of surfactant was ideal for enhanced incorporation of drugs within transferosomes. The percentage entrapment and loading efficiencies of EGCG-TRANS and AA-TRANS were 76.11 ± 3.3 and 80.13 ± 3.9 and 14.01 ± 0.5 and 16.34 ± 2.8, respectively. The percentage entrapment and loading efficiencies of EGCG-AA-TRANS were 82.27 ± 4.8 and 15.08 ± 1.5 and 74.81 ± 4.1 and 12.51 ± 1.7, respectively, for AA and EGCG (Table 1). The hydrodynamic particle sizes of the prepared transferosome were observed to be 174.2 ± 1.8, 132.7 ± 12.22, and 184.31 ± 9.5 for EGCG-TRANS, AA-TRANS, and EGCG-AA-TRANS, respectively. ζ is a crucial parameter that indicates the density of the surface charge on nanoparticles, influencing their adhesion and transport properties. A negative ζ is typically associated with the stability of transferosomes.[41,42] In the present study, no ionization chain attached to the transferosome leads to a low ζ value. The negative ζ value suggests successful incorporation of epigallocatechin and AA within the transferosomes. ζ was observed in EGCG-TRANS, AA-TRANS, and EGCG-AA-TRANS (-19.13 ± 0.41, -22.14 ± 0.98, and -14.21 ± 0.01).

3.23.2. Scanning electron microscopy. SEM images showed an increased particle size of the AA and-EGCG loaded transferosome, conforming successful drug loading.[43] SEM images of EGCG-TRANS, AA-TRANS, and EGCG-AA-TRANS vesicles are shown in Figure 3. The vesicle sizes of EGCG-AA-TRANS, EGCG-TRANS, and AA-TRANS were found to be 182.82 ± 10.5, 172.25 ± 3.5, and 131.43 ± 12.12 nm, respectively.
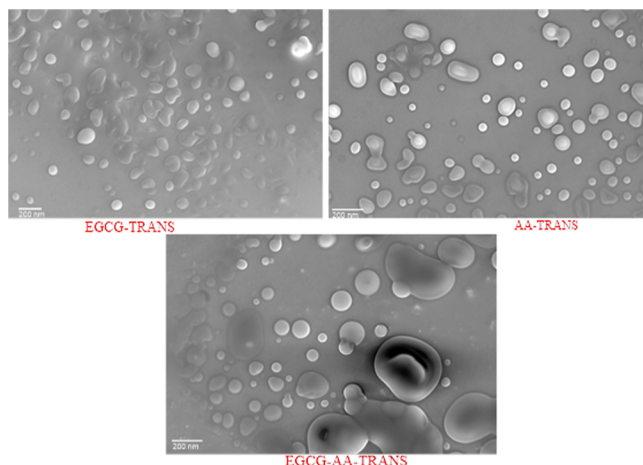

Figure 3. SEM images of the prepared transferosome.

3.3. Atomic Force microscopy. AFM images show important information about the transferosomes' surface topography, which is important for understanding how they interact with biological parts and how they could be used for drug delivery or other purposes. On a smooth surface, transferosomes may have enhanced stability and reduced chances of aggregation. AFM images produce 2D and 3D images of transferosomes and provide surface details in the nanometer range. Minimal surface roughness suggested the existence of a surface lipid.[44] The vesicles had a roughness average (Rq) of 4.976 nm and a root-mean-square (Ra) of 7.654 nm (Figure 4). This showed that the vesicles had a smooth surface.

3.4. Hemolytic Toxicity Study. Hemolytic toxicity assessment was done to ensure the biosafety of formulations. The results showed 10.23, 7.21, and 8.20% of hemolysis for EGCG-TRANS, AA-TRANS, and EGCG-AA-TRANS, respectively (Figure 5). Hemolysis results indicated the safety of the vesicles. Formulations with a hemolysis value of <10% are nonhemolytic, whereas values > 25% indicate the risk of hemolysis. This implies that these formulations use a safer delivery system to transport the bioactive compounds.[45,46]

3.5. Drug Release Study. The drug release study results demonstrate a sustained release pattern of the compounds from the formulations, suggesting the potential to enhance the therapeutic effectiveness of the loaded drugs.[47] In vitro release of EGCG and AA from EGCG-TRANS, AA-TRANS, and EGCG-AA-TRANS formulations was examined in 100 mL of PBS (pH 7.4) utilizing the dialysis bag technique over a duration of 72 h. Over the initial 24 h period, the EGCG release from EGCG-TRANS was measured at $84.09\% \pm 2.09$, while the release of AA from AA-TRANS was $88.43\% \pm 3.07$. In the case of EGCG-AA-TRANS, the release of EGCG was determined to be $61.65\% \pm 4.61$ after 72 h (Figure 6).

3.6. Acetylcholinesterase Activity. EGCG-AA-TRANS showed improved and effective AChE inhibition activity. Inhibiting AChE reduces acetylcholine breakdown, potentially increasing acetylcholine levels in the brain and enhancing cognitive function.[48] Figure 7 shows that EGCG-AA-TRANS (82.166%) exhibited a higher percentage of AChE activity in comparison to EGCG-TRANS (66.550%) and AA-TRANS (53.466%). EGCG inhibits the aggregation of beta-amyloid proteins, which form plaques in the brains of Alzheimer's patients.[13] AA, on the other hand, can enhance the clearance of beta-amyloid from the brain and increase the bioavailability of EGCG by stabilizing its molecular structure.[14] This could be a possible reason for the synergistic inhibition activity of EGCG-AA-TRANS.

3.7. In Vivo Assay. *3.7.1. Behavioral Assay. 3.7.1.1. Morris Water Maze Test.* Scopolamine dosing reduced the spatial memory of mice. However, it was improved in treated mice with EGCG-TRANS, AA-TRANS, and EGCG-AA-TRANS by 16 ($p < 0.001$), 20 ($p < 0.001$), and 20 ($p < 0.001$), respectively. The number of entries in the arm was highest in the control group, at 38 ($p < 0.001$) times, and lowest in the scopolamine group, at about 12 ($p < 0.001$) times. EGCG and AA-treated mice showed significant improvement, with 14 ($p < 0.001$) and 15 ($p < 0.001$) times of entries in the arm, respectively. In this study, scopolamine-treated mice took more time (84 s) to find the hidden acrylic platform than the control group (26 s, $p < 0.001$). The time required by the mice treated with pure EGCG (42 s), AA (38 s), EGCG-TRANS (46 s), AA-TRANS (39 s), and EGCG-AA-TRANS (24 s) was significantly ($p < 0.001$) less than that of the AD group (84 s) (Figure 8A). On the fifth day, after platform removal, the probe test showed that the negative control AD mice group spent less time in the target quadrant and more time in other quadrants when compared to the control, EGCG, AA, EGCG-TRANS, AA-TRANS, and EGCG-AA-TRANS-treated groups. Dosing mice with scopolamine significantly reduced their spatial memory, while animals treated with EGCG, AA, EGCG-TRANS, AA-TRANS, and EGCG-AA-TRANS showed improved spatial memory (Figure 8B).

3.7.1.2. Y-Maze Test. Scopolamine dosing significantly reduced the spatial memory of mice because of the cognitive decline associated with the hippocampus. A natural compound
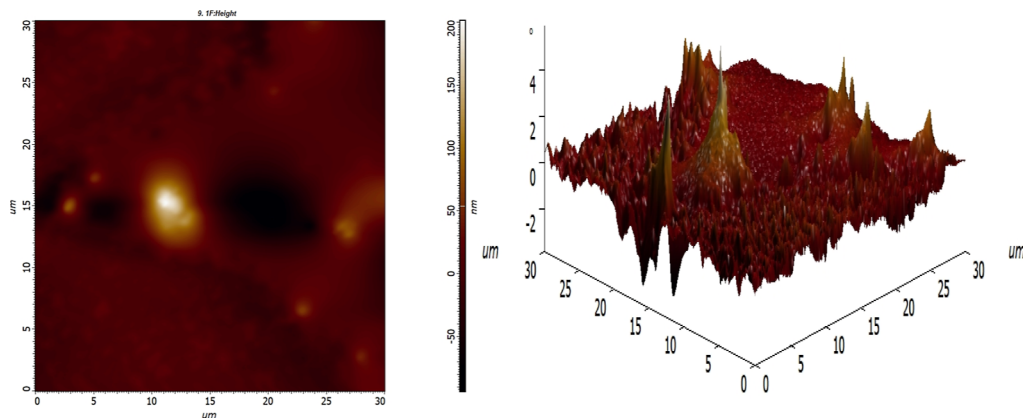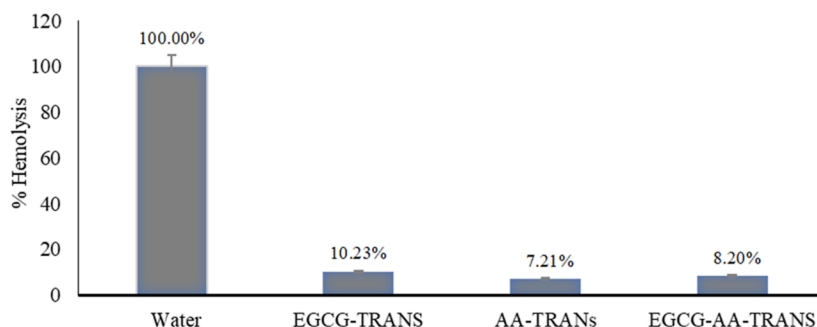
Figure 4. AFM images of EGCG-AA-TRANS (2D and 3 D).

Figure 5. Percentage of RBC rupture compared to pure water in transferosomes (mean $\pm$ SD, n = 3).
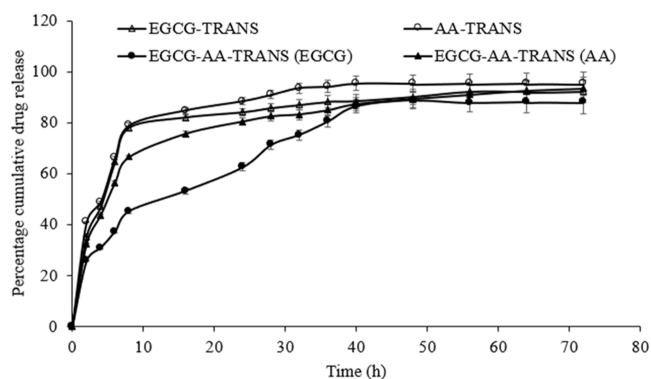

Figure 6. Release profile of the prepared transferosomes of epigallocatechin-3-gallate and AA (empty triangles: EGCG release from EGCG-TRANS, empty circles: AA release from AA-TRANS, filled circles: EGCG release from EGCG-AA-TRANS, and filled triangles: AA release from EGCG-AA-TRANS) in PBS (pH 7.4) (mean $\pm$ SD, n = 3).

Figure 7. Percent AChE activities with inhibitors obtained at 412 nm: (A) EGCG-TRANS, (B) AA-TRANS, and (C) EGCG-AA-TRANS (mean $\pm$ SEM, n = 5). Statistical analysis was carried out using a one-way ANOVA, followed by the Newman−Keuls test (p < 0.001).

found in green tea and AA (a natural antioxidant) as a treatment or intervention in the Y-maze test. Animal models have shown that giving EGCG and AA together has a greater effect than giving them separately, without causing any toxic behavior.[49] The decrease in latency time across repeated trials indicates improved spatial memory performance. Numerous studies have widely recognized and employed this test to investigate memory and learning capabilities in animals and humans.[50] It involves observing the time it takes for a subject to find a hidden platform submerged in a pool of water. In the Y-maze test, scopolamine treatment reduced the spatial memory of mice due to the cognitive decline associated with the hippocampus. EGCG has been explored for its potential
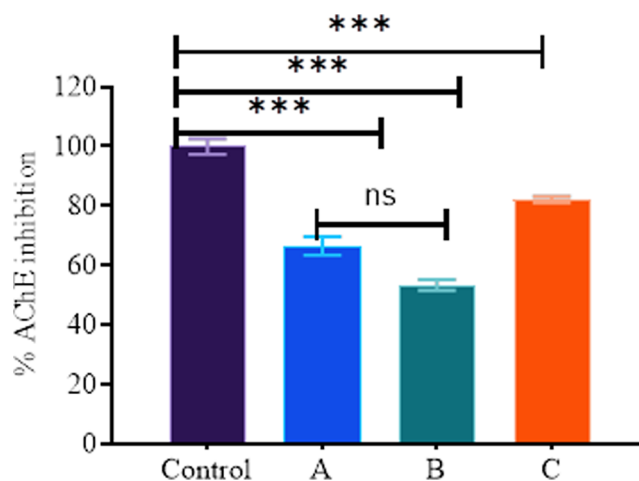
neuroprotective and cognitive-enhancing properties.[51] The spatial memory of mice was significantly reduced due to scopolamine treatment. However, it was enhanced in mice treated with EGCG-TRANS, AA-TRANS, and EGCG-AA-TRANS by 16 (p <0.001), 20 (p <0.001), and 20 (p <0.001), respectively (Figure 9).

3.8. Biochemical Assay. *3.8.1. SOD and Catalase Activity.* Reactive oxygen species levels in the hippocampus were assessed by measuring the level of antioxidant enzymes like SOD and catalase. EGCG and AA influenced the activity of these antioxidant enzymes. EGCG-AA-TRANS showed a
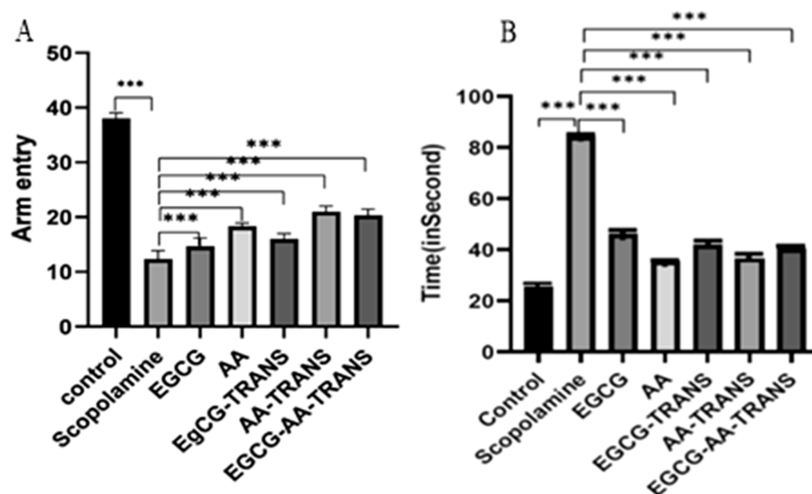
Figure 8. Results of behavioral analysis in the Morris water-maze test: (A) entries in arms and (B) time spent on the hidden platform as shown by the treated groups (mean $\pm$ SEM, $n = 5$). Statistical analysis was carried out using one-way ANOVA, followed by the Newman–Keuls test ($p < 0.001$).
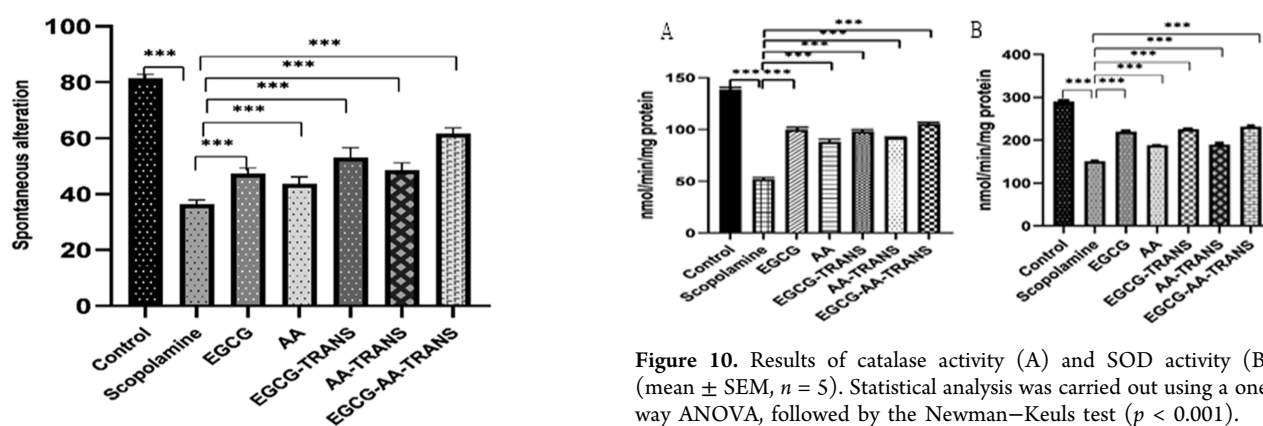

Figure 9. Results of behavioral study in Y-maze test: spontaneous alteration shown by the EGCG, AA, EGCG-TRANS, AA-TRANS, and EGCG-AA-TRANS in mice (mean $\pm$ SEM, $n = 5$). Statistical analysis was carried out using one-way ANOVA, followed by the Newman–Keuls test ($p < 0.001$).

Figure 10. Results of catalase activity (A) and SOD activity (B) (mean $\pm$ SEM, $n = 5$). Statistical analysis was carried out using a one-way ANOVA, followed by the Newman–Keuls test ($p < 0.001$).

higher level of modulation in antioxidant enzyme activity. However, it showed the most significant effect. The SOD activity in the hippocampus of mice with AD was markedly reduced compared to the control group ($p < 0.001$). Therefore, when administering EGCG-TRANS, AA-TRANS, or EGCG-AA-TRANS to scopolamine-intoxicated mice, a notable restoration in catalase levels was observed ($p < 0.001$) due to their antioxidative properties. The observed catalase activities by EGCG-TRANS, AA-TRANS, and EGCG-AA-TRANS were 41.73, 36.54, and 40.25 nmol/min/mg protein, respectively (Figure 10A).[52,53] Moreover, in scopolamine-induced animals, the SOD activity was significantly improved compared to the control group. The observed SOD activities by EGCG-TRANS, AA-TRANS, and EGCG-AA-TRANS were 85.98, 94.31, and 107.38 nmol/min/mg protein, respectively (Figure 10B). Interestingly, EGCG-AA-TRANS-treated animals showed a slight reduction in SOD activity compared to the control group. The mice that had been injected with scopolamine had much lower SOD activity ($p < 0.001$) than the mice that had been given pure drugs or the drug-loaded transferosomes.[52]

3.9. Lipid Peroxidation. In the lipid peroxidation test, MDA levels were measured to find out how EGCG, AA, EGCG-TRANS, AA-TRANS, and EGCG-AA-TRANS affected lipid peroxidation levels in the hippocampus tissue homogenate of mice with AD. Reports indicate elevated levels of MDA in mouse models of AD, indicating a compromised defense against oxidative stress. Free radicals that are reactive can damage the structure and function of phospholipids in cell membranes. This can lead to lipid peroxidation and the creation of byproducts such as MDA. This compound serves as a biomarker for lipid peroxidation in the periphery, indicating potential oxidative damage in AD patients.[54] A higher level of MDA in the hippocampus and lower levels of MDA in AD mice showed potential beneficial effects of treatments in mitigating lipid peroxidation in the hippocampus of AD mice.[55] The results revealed that AD mice exhibited a significant increase in malondialdehyde levels in the hippocampus compared to the control group ($p < 0.01$) (Figure 11). Also, mice with AD who were given EGCG-TRANS, AA-TRANS, and EGCG-AA-TRANS had much lower levels of MDA than mice with AD who were given scopolamine ($p < 0.001$).

3.10. NO Test. In the hippocampus tissue homogenate of AD mice given scopolamine, NO levels were significantly higher ($p < 0.001$) than in the control group. However, treatment with EGCG and AA resulted in a significant decrease
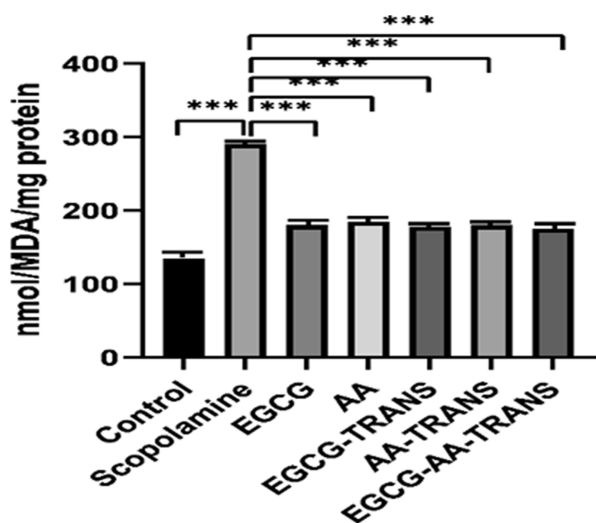
Figure 11. Results shown for lipid peroxidation test by treated groups (mean ± SEM, $n = 5$). Statistical analysis was carried out using a one-way ANOVA followed by the Newman−Keuls test ($p < 0.001$).

in NO levels. Furthermore, the administration of EGCG-TRANS and AA-TRANS also led to a considerable reduction in NO levels in AD mice (Figure 12). When compared to scopolamine-induced AD mice, the EGCG-AA-TRANS-treated group recorded the most substantial reduction in NO levels.[56]
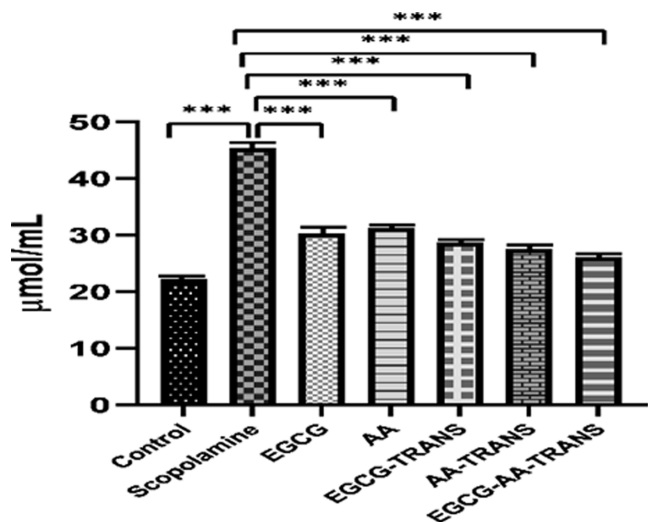

Figure 12. Results shown by the nitrite test in treated groups (mean ± SEM, $n = 5$). Statistical analysis was carried out using a one-way ANOVA followed by the Newman−Keuls test ($p < 0.001$).

3.11. Organ Distribution Study. Transferosomes resulted in higher drug concentrations in the brain. The enhanced penetration and ultraflexible structure of transferosomes, used for nose-to-brain delivery, may be responsible for this improvement. Even though the concentration of drugs in the brain is less than that in the liver, overall enhanced drug distribution is observed because of the nasal-to-brain delivery and small particles easily distributed to the brain.[57,58] The concentration of the drug in the brains of animals treated with EGCG-AA-TRANS was higher compared to the pure drug solution. The mean residence time of EGCG-AA-TRANS in the brain tissue was five times higher, suggesting an increased

retention of transferosome vesicles in the mice brain. The prolonged residence period could be ascribed to the transferosomes' superior penetration and incredibly flexible nature, which enable effective nose-to-brain distribution.[58] The administration of EGCG-AA-TRANS improved drug concentrations in the brain (Figure 13). The concentration of drugs in the brain was less than that in the liver.
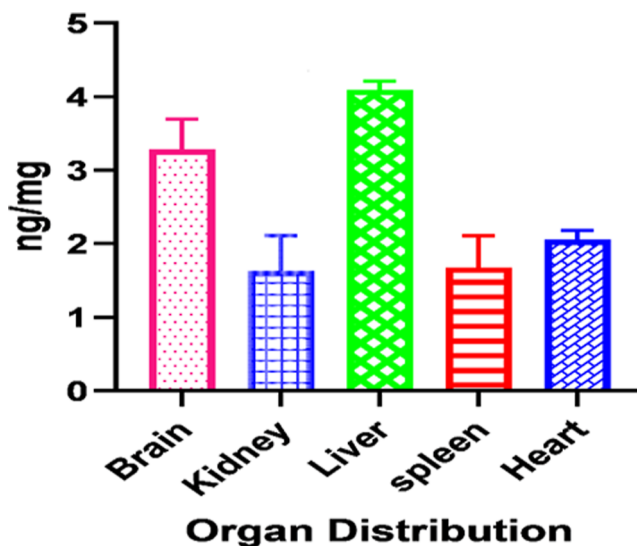

Figure 13. Organ distribution study of EGCG-AA-TRANS (mean ± SEM, $n = 5$).

3.12. Hematological Study. The animals treated with EGCG-TRANS and EGCG-AA-TRANS showed $6.65 \pm 0.07 \times 10^{-6}$ and $7.63 \pm 0.01 \times 10^{-6}$ μL^{-1} RBC count, respectively. In control and AA-TRANS-treated mice, the RBC count was $7.67 \pm 0.41 \times 10^{-6}$ and $6.7 \pm 0.21 \times 10^{6}$ μL^{-1}, respectively (Table 2). The hemoglobin level in the control and EGCG-TRANS-treated groups was 11.90 ± 0.72 g/dL. The hemoglobin levels in mice treated with AA-TRANS and EGCG-AA-TRANS-treated were 12.2 ± 0.02 and 13.01 ± 0.07, respectively. The WBC count in EGCG-TRANS and AA-TRANS was observed at 5.94 ± 0.22 and 4.91 ± 0.41, respectively, and in EGCG-AA-TRANS was 6.49 ± 0.12.[57]

3.13. Estimation of ECGC and AA in the Brain and Their Kinetic Profile. The concentration of the drug in the brains of animals treated with EGCG-AA-TRANS was found to be higher compared to those that received the pure drug solution. This indicates that the prepared formulation exhibited a greater ability to transport the drug to the brain. Additionally, the mean residence time in the brain tissue of EGCG-AA-TRANS (5.321 ± 0.124 h)-treated animals was observed to be five times higher in comparison to EGCG (1.4 ± 0.985) and AA plain (Table 3).

4. CONCLUSIONS

The compound epigallocatechin-3-gallate (EGCG) has shown promise as a potential treatment for AD. However, its instability limits its effectiveness and bioavailability. To address this, we formulated EGCG as a dual-drug-loaded EGCG and AA-loaded transferosome, which increased its synergistic effect. When administered nasally to mice, EGCG-AA-TRANS led to a higher accumulation of EGCG in major organs, including the brain. After nasal administration, the pharmacokinetics of free

Table 2. Results Shown for Hematological Parameters Study in Blood of Treated Groups with Transferosomal Formulations (Mean ± SD, n = 5)

blood parameter	control (blank)	EGCG-TRANS	AA-TRANS	EGCG-AA-TRANS
WBCs ($\times 10^3 \ \mu L^{-1}$)	6.34 ± 2.2	5.94 ± 0.22	4.91 ± 0.41	6.49 ± 0.12
RBCs ($\times 10^6 \ \mu L^{-1}$)	7.67 ± 0.41	6.65 ± 0.07	6.7 ± 0.21	7.63 ± 0.01
Hb (g/dL)	11.90 ± 0.72	11.65 ± 0.61	12.2 ± 0.02	13.01 ± 0.07

Table 3. Results of in Vivo Pharmacokinetic Study of EGCG and AA in Brain of Treated Groups with Transferosomal Formulations (Mean ± SD, n = 5)

samples	AUC_{0-24} (ng × h/mL)	C_{max} (ng/L)	T_{max} (h)	MRT_{0-24} (h)
EGCG	1123.300 ± 0.0.432	786.07 ± 0.784	1.101 ± 2.871	1.412 ± 0.985
AA	1060.980 ± 0.654	855.030 ± 0.654	2.122 ± 0.871	1.983 ± 0.121
EGCG-TRANS	2144.070 ± 0.442	1285.320 ± 0.650	3.000 ± 0.231	4.123 ± 0.214
AA-TRANS	1430.030 ± 0.786	1222.550 ± 0.643	2.032 ± 0.112	4.918 ± 0.769
EGCG-AA-TRANS	2550.540 ± 0.432	1310.320 ± 0.032	5.098 ± 0.451	5.321 ± 0.124

EGCG, AA, and EGCG-AA-TRANS were compared. The initial EGCG concentrations were similar in both cases, but the long-term concentrations were about 5 times higher with EGCG-AA-TRANS. The mechanism behind this enhancement is linked to a specific BBB pathway. In a mouse model of AD, nasal treatment with EGCG-AA-TRANS led to several positive outcomes, such as increased AChE activity and neuro-inflammation. These changes were accompanied by improved spatial learning and memory. Thus, the stabilization of EGCG in nanoparticle complexes and the destabilization of the BBB contributed to higher therapeutic EGCG concentrations in the brain. This suggests developing EGCG-AA-TRANS as a safe and effective strategy for treating AD.

AUTHOR INFORMATION

Corresponding Author

Manmath K. Nandi − *Department of Medicinal Chemistry, Institute of Medical Sciences, Banaras Hindu University, Varanasi 221005 Uttar Pradesh, India;* orcid.org/0000-0001-8901-8538; Email: manmath.nandi@gmail.com

Authors

Gaurav Mishra − *Department of Medicinal Chemistry, Institute of Medical Sciences, Banaras Hindu University, Varanasi 221005 Uttar Pradesh, India;* orcid.org/0000-0002-8969-0014

Rajendra Awasthi − *Department of Pharmaceutical Sciences, School of Health Sciences and Technology, UPES, Dehradun 248007 Uttarakhand, India;* orcid.org/0000-0002-1286-1874

Sunil Kumar Mishra − *Department of Pharmaceutical Engineering & Technology, Indian Institute of Technology (Banaras Hindu University), Varanasi 221005 Uttar Pradesh, India*

Anurag Kumar Singh − *Centre of Experimental Medicine & Surgery, Institute of Medical Sciences, Banaras Hindu University, Varanasi 221005 Uttar Pradesh, India;* orcid.org/0000-0003-2125-810X

Anurag Kumar Tiwari − *Department of Gastroenterology, Institute of Medical Sciences, Banaras Hindu University, Varanasi 221005 Uttar Pradesh, India*

Santosh Kumar Singh − *Centre of Experimental Medicine & Surgery, Institute of Medical Sciences, Banaras Hindu University, Varanasi 221005 Uttar Pradesh, India;* orcid.org/0000-0001-6521-7719

Complete contact information is available at:
https://pubs.acs.org/10.1021/acsomega.4c02140

REFERENCES

(1) Cummings, J.; Isaacson, R.; Schmitt, F.; Velting, D. A practical algorithm for managing Alzheimer's disease: what, when, and why? *Ann. Clin. Transl. Neurol.* **2015**, *2*, 307−323.

(2) Alzheimer's Association. Alzheimer's disease facts and figures. *Alzheimer's Dementia* **2017**, *13* (4), 325−373.

(3) Nandi, A.; Counts, N.; Bröker, J.; Malik, S.; Chen, S.; Han, R.; Klusty, J.; Seligman, B.; Tortorice, D.; Vigo, D.; Bloom, D. E. Cost of care for Alzheimer's disease and related dementias in the United States: 2016 to 2060. *npj Aging* **2024**, *10* (1), 13.

(4) Ballard, C.; Gauthier, S.; Corbett, A.; Brayne, C.; Aarsland, D.; Jones, E. Alzheimer's disease. *Lancet* **2011**, *377* (9770), 1019−1031.

(5) Cabrera, C.; Artacho, R.; Giménez, R. Beneficial effects of green tea—a review. *J. Am. Coll. Nutr.* **2006**, *25*, 79−99.

(6) Khan, N.; Mukhtar, H. Tea and health: studies in humans. *Curr. Pharm. Des.* **2013**, *19*, 6141−6147.

(7) Khan, N.; Mukhtar, H. Tea Polyphenols in Promotion of Human Health. *Nutrients* **2018**, *11*, No. E39.

(8) Shi, X.; Lin, X.; Hu, R.; Sun, N.; Hao, J.; Gao, C. Toxicological differences between NMDA receptor antagonists and cholinesterase inhibitors. *Am. J. Alzheimers Dis. Other Demen.* **2016**, *31* (5), 405−412.

(9) Chacko, S. M.; Thambi, P. T.; Kuttan, R.; Nishigaki, I. Beneficial effects of green tea: a literature review. *Chin. Med.* **2010**, *5*, 13.

(10) Yi, M.; Wu, X.; Zhuang, W.; Xia, L.; Chen, Y.; Zhao, R.; Wan, Q.; Du, L.; Zhou, Y. Tea Consumption and Health Outcomes: Umbrella Review of Meta-Analyses of Observational Studies in Humans. *Mol. Nutr. Food Res.* **2019**, *63*, No. e1900389.

(11) Valverde-Salazar, V.; Ruiz-Gabarre, D.; García-Escudero, V. Alzheimer's disease and green tea: epigallocatechin-3-gallate as a modulator of inflammation and oxidative stress. *Antioxidants* **2023**, *12* (7), 1460.

(12) Semwal, B. C.; Singh, B.; Murti, Y.; Singh, S. Therapeutic Potential of Ascorbic Acid in the Management of Alzheimer's Disease: An Update. *Curr. Pharm. Biotechnol.* **2023**, *25* (2), 196−212.

(13) Shimmyo, Y.; Kihara, T.; Akaike, A.; Niidome, T.; Sugimoto, H. Epigallocatechin-3-gallate and curcumin suppress amyloid beta-induced beta-site APP cleaving enzyme-1 upregulation. *Neuroreport* **2008**, *19* (13), 1329−1333.

(14) Xie, Q.; Cai, X.; Dong, X.; Wang, Y.; Sun, M.; Tai, L.; Xu, Y. Effects of epigallocatechin-3-gallate combined with ascorbic acid and glycerol on the stability and uric acid-lowering activity of epigallocatechin-3-gallate. *Pharmaceut. Biol.* **2021**, *59* (1), 155−164.

(15) Singh, S.; Awasthi, R. Berberine HCl and diacerein loaded dual delivery transferosomes: Formulation and optimization using Box-Behnken design. *ADMET and DMPK* **2024**.

(16) Mirza, R.; Khan, A. U.; Shah, K. U.; Ullah, N.; Nawaz, A.; Ghani, S. F.; Javed, A.; Shah, S. U.; Alasmari, A. F.; Alharbi, M.; Alasmari, F.; et al. Brain targeting of cefepime loaded transfersomes based thermosensitive in situ gel via intranasal delivery: In vitro and in vivo studies. *J. Drug Delivery Sci. Technol.* **2024**, *95*, 105585.

(17) Salem, H. F.; Aboud, H. M.; Abdellatif, M. M.; Abou-Taleb, H. A. Nose-to-Brain Targeted Delivery of Donepezil Hydrochloride via Novel Hyaluronic Acid-Doped Nanotransfersomes for Alzheimer's Disease Mitigation. *J. Pharm. Sci.* **2024**.

(18) Gupta, I.; Adin, S. N.; Aqil, M.; Mujeeb, M. Nose to brain delivery of naringin loaded transniosomes for epilepsy: formulation, characterisation, blood-brain distribution and *in vivo* pharmacodynamic evaluation. *J. Liposome Res.* **2024**, *34* (1), 60−76.

(19) Mishra, G.; Awasthi, R.; Singh, A. K.; Singh, S.; Mishra, S. K.; Singh, S. K.; Nandi, M. K. Intranasally Co-administered Berberine and Curcumin Loaded in Transfersomal Vesicles Improved Inhibition of Amyloid Formation and BACE-1. *ACS Omega* **2022**, *7* (47), 43290−43305.

(20) Wang, G.; Maciel, D.; Wu, Y.; Rodrigues, J.; Shi, X.; Yuan, Y.; Liu, C.; Tomás, H.; Li, Y. Amphiphilic polymer-mediated formation of laponite-based nanohybrids with robust stability and pH sensitivity for anticancer drug delivery. *ACS Appl. Mater. Interfaces* **2014**, *6*, 16687−16695.

(21) Bhadra, D.; Bhadra, S.; Jain, S.; Jain, N. K. A PEGylated dendritic nanoparticulate carrier of fluorouracil. *Int. J. Pharm.* **2003**, *257*, 111−124.

(22) Singh, A. K.; Singh, S. S.; Rathore, A. S.; Singh, S. P.; Mishra, G.; Awasthi, R.; Mishra, S. K.; Gautam, V.; Singh, S. K. Lipid-coated MCM-41 mesoporous silica nanoparticles loaded with berberine improved inhibition of acetylcholine esterase and amyloid formation. *ACS Biomater. Sci. Eng.* **2021**, *7*, 3737−3753.

(23) Vladár, A. E.; Hodoroaba, V. D. Characterization of nanoparticles by scanning electron microscopy. In *Characterization of Nanoparticles*; Elsevier, 2020; pp 7−27.

(24) Zheng, J. P.; Luan, L.; Wang, H. Y.; Xi, L. F.; Yao, K. D. Study on ibuprofen/ montmorillonite intercalation composites as drug release system. *Appl. Clay Sci.* **2007**, *36*, 297−301.

(25) Pandey, P. K.; Sharma, A. K.; Rani, S.; Mishra, G.; Kandasamy, G.; Patra, A. K.; Rana, M.; Sharma, A. K.; Yadav, A. K.; Gupta, U. MCM-41 nanoparticles for brain delivery: better choline-esterase and amyloid formation inhibition with improved kinetics. *ACS Biomater. Sci. Eng.* **2018**, *4* (8), 2860−2869.

(26) Dobrovolskaia, M. A.; Clogston, J. D.; Neun, B. W.; Hall, J. B.; Patri, A. K.; McNeil, S. E. Method for analysis of nanoparticle hemolytic properties in vitro. *Nano Lett.* **2008**, *8* (8), 2180−2187.

(27) Chen, P. J.; Liang, K. C.; Lin, H. C.; Hsieh, C. L.; Su, K. P.; Hung, M. C.; Sheen, L. Y. Gastrodiaelata Bl. Attenuated learning deficits induced by forced-swimming stress in the inhibitory avoidance task and Morris water maze. *J. Med. Food* **2011**, *14* (6), 610−617.

(28) Zhang, L.; Fang, Y.; Xu, Y.; Lian, Y.; Xie, N.; Wu, T.; Zhang, H.; Sun, L.; Zhang, R.; Wang, Z. Curcumin Improves Amyloid *β*-Peptide (1-42) Induced Spatial Memory Deficits through BDNF-ERK Signaling Pathway. *PLoS One* **2015**, *10*, No. e0131525.

(29) Singh, S. S.; Rai, S. N.; Birla, H.; Zahra, W.; Kumar, G.; Gedda, M. R.; Tiwari, N.; Patnaik, R.; Singh, R. K.; Singh, S. P. Effect of Chlorogenic Acid Supplementation in MPTP-Intoxicated Mouse. *Front. Pharmacol* **2018**, *9*, 757.

(30) Misra, H. P.; Fridovich, I. The Role of Superoxide Anion in the Autoxidation of Epinephrine and a Simple Assay for Superoxide Dismutase. *J. Biol. Chem.* **1972**, *247*, 3170−3175.

(31) Ohkawa, H.; Ohishi, N.; Yagi, K. Assay for lipid peroxides in animal tissues by thiobarbituric acid reaction. *Anal. Biochem.* **1979**, *95* (2), 351−358.

(32) Anstey, N. M.; Weinberg, J. B.; Hassanali, M. Y.; Mwaikambo, E. D.; Manyenga, D.; Misukonis, M. A.; Arnelle, D. R.; Hollis, D.; McDonald, M. I.; Granger, D. L. Nitric oxide in Tanzanian children with malaria: inverse relationship between malaria severity and nitric oxide production/nitric oxide synthase type 2 expression. *J. Exp. Med.* **1996**, *184* (2), 557−567.

(33) Misra, H. P.; Fridovich, I. The role of superoxide anion in the autoxidation of epinephrine and a simple assay for superoxide dismutase. *J. Biol. Chem.* **1972**, *247* (10), 3170−3175.

(34) Loryan, I.; Friden, M.; Hammarlund-Udenaes, M. The brain slice method for studying drug distribution in the CNS. *Fluids Barriers CNS* **2013**, *10*, 6.

(35) Wavikar, P.; Pai, R.; Vavia, P. Nose to brain delivery of rivastigmine by in situ gelling cationic nanostructured lipid carriers: enhanced brain distribution and pharmacodynamics. *J. Pharm. Sci.* **2017**, *106*, 3613−3622.

(36) Kulhari, H.; Pooja, D.; Prajapati, S. K.; Chauhan, A. S. Performance evaluation of PAMAM dendrimer based simvastatin formulations. *Int. J. Pharm.* **2011**, *405*, 203−209.

(37) Bhadra, D.; Yadav, A. K.; Bhadra, S.; Jain, N. K. Glycodendrimeric nanoparticulate carriers of primaquine phosphate for liver targeting. *Int. J. Pharm.* **2005**, *295*, 221−233.

(38) Raval, N.; Maheshwari, R.; Kalyane, D.; Youngren-Ortiz, S. R.; Chougule, M. B.; Tekade, R. K. Importance of physicochemical characterization of nanoparticles in pharmaceutical product development. In: *Basic Fundamentals of Drug Delivery*, 1st ed.; Tekade, R. K., Ed.; Elsevier Academic Press: San Diego CA, 2018; pp 369−400.

(39) Nii, T.; Ishii, F. Encapsulation efficiency of water-soluble and insoluble drugs in liposomes prepared by the microencapsulation vesicle method. *Int. J. Pharm.* **2005**, *298*, 198−205.

(40) Barenholz, Y. Relevancy of drug loading to liposomal formulation therapeutic efficacy. *J. Liposome Res.* **2003**, *13*, 1−8.

(41) Tang, D. W.; Yu, S. H.; Ho, Y. C.; Huang, B. Q.; Tsai, G. J.; Hsieh, H. Y.; Sung, H. W.; Mi, F. L. Characterization of tea catechins-loaded nanoparticles prepared from chitosan and an edible polypeptide. *Food Hydrocolloids* **2013**, *30*, 33−41.

(42) Muller, R. H.; Jacobs, C.; Kayser, O. Nanosuspensions as particulate drug formulations in therapy. *Adv. Drug Delivery Rev.* **2001**, *47*, 3−19.

(43) Zeng, L.; Yan, J.; Luo, L.; Ma, M.; Zhu, H. Preparation and characterization of (−)-Epigallocatechin-3-gallate (EGCG)-loaded nanoparticles and their inhibitory effects on Human breast cancer MCF-7 cells. *Sci. Rep.* **2017**, *7* (1), 45521.

(44) Kazi, J.; Sen, R.; Ganguly, S.; Jha, T.; Ganguly, S.; Chatterjee Debnath, M. Folate decorated epigallocatechin-3-gallate (EGCG) loaded PLGA nanoparticles; in-vitro and in-vivo targeting efficacy against MDA-MB-231 tumor xenograft. *Int. J. Pharm.* **2020**, *585*, 119449.

(45) Ran, Q.; Xiang, Y.; Liu, Y.; Xiang, L.; Li, F.; Deng, X.; Xiao, Y.; Chen, L.; Chen, L.; Li, Z. Eryptosis indices as a novel predictive parameter for biocompatibility of Fe3O4 magnetic nanoparticles on erythrocytes. *Sci. Rep.* **2015**, *5*, 16209.

(46) Amin, K.; Dannenfelser, R. M. In vitro hemolysis: Guidance for the pharmaceutical scientist. *J. Pharm. Sci.* **2006**, *95*, 1173−1176.

(47) Son, G. H.; Lee, B. J.; Cho, C. W. Mechanisms of drug release from advanced drug formulations such as polymeric-based drug-delivery systems and lipid nanoparticles. *J. Pharm. Invest.* **2017**, *47*, 287−296.

(48) Lin, Y.; Wang, Y.; Lv, J.; Wang, N.; Wang, J.; Li, M. Targeted acetylcholinesterase-responsive drug carriers with long duration of drug action and reduced hepatotoxicity. *Int. J. Nanomed.* **2019**, *14*, 5817−5829.

(49) Varma, R. K.; Singh, L.; Garg, V. K.; Yadav, P.; Singh, V. K. Nootropic effect of Vigna Mungo (L.) hpper seeds extract in scopalamine induced amnesic rats. *World J. Pharm. Pharmaceut. Sci.* **2016**, *5*, 1176−1192.

(50) Lee, Y. J.; Choi, D. Y.; Yun, Y. P.; Han, S. B.; Oh, K. W.; Hong, J. T. Epigallocatechin-3-gallate prevents systemic inflammation-induced memory deficiency and amyloidogenesis via its anti-neuroinflammatory properties. *J. Nutr. Biochem.* **2013**, *24* (1), 298−310.

(51) Mori, T.; Koyama, N.; Tan, J.; Segawa, T.; Maeda, M.; Town, T. Combined treatment with the phenolics (−)-epigallocatechin-3-gallate and ferulic acid improves cognition and reduces Alzheimer-like pathology in mice. *J. Biol. Chem.* **2019**, *294* (8), 2714−5444.

(52) Song, S.; Huang, Y. W.; Tian, Y.; Wang, X. J.; Sheng, J. Mechanism of action of (−)-epigallocatechin-3-gallate: auto-oxidation-dependent activation of extracellular signal-regulated kinase 1/2 in Jurkat cells. *Chin. J. Nat. Med.* **2014**, *12* (9), 654−662.

(53) Miyake, N.; Kim, M.; Kurata, T. Stabilization of L-ascorbic acid by superoxide dismutase and catalase. *Biosci., Biotechnol., Biochem.* **1999**, *63* (1), 54−57.

(54) Hurşitoğlu, O.; Orhan, F. Ö.; Kurutaş, E. B.; Doğaner, A.; Durmuş, H. T.; Kopar, H. Diagnostic performance of increased malondialdehyde level and oxidative stress in patients with schizophrenia. *Arch. Neuropsychiatry* **2021**, *58* (3), 184.

(55) Ostrowska, J.; Łuczaj, W.; Kasacka, I.; Różański, A.; Skrzydlewska, E. Green tea protects against ethanol-induced lipid peroxidation in rat organs. *Alcohol* **2004**, *32* (1), 25−32.

(56) Zhang, Z.; Zhang, D. (−)-Epigallocatechin-3-gallate inhibits eNOS uncoupling and alleviates high glucose-induced dysfunction and apoptosis of human umbilical vein endothelial cells by PI3K/AKT/eNOS pathway. *Diabetes, Metab. Syndr. Obes.: Targets Ther.* **2020**, *Volume 13*, 2495−2504.

(57) Singh, A. K.; Mishra, S. K.; Mishra, G.; Maurya, A.; Awasthi, R.; Yadav, M. K.; Atri, N.; Pandey, P. K.; Singh, S. K. Inorganic clay nanocomposite system for improved cholinesterase inhibition and brain pharmacokinetics of donepezil. *Drug Dev. Ind. Pharm.* **2020**, *46* (1), 8−19.

(58) Cano, A.; Ettcheto, M.; Chang, J.; Barroso, E.; Espina, M.; Kühne, B. A.; Barenys, M.; Auladell, C.; Folch, J.; Souto, E. B.; Camins, A.; et al. Dual-drug loaded nanoparticles of Epigallocatechin-3-gallate (EGCG)/Ascorbic acid enhance therapeutic efficacy of EGCG in a APPswe/PS1dE9 Alzheimer's disease mice model. *J. Controlled Release* **2019**, *301*, 62−75.